

# The antiferromagnetic/paramagnetic transition in mixed-spin compounds $R_2\text{BaNiO}_5$

J.V. Alvarez<sup>1</sup> and Roser Valentí<sup>2</sup>

<sup>1</sup> Department of Physics, University of Michigan, Ann Arbor 48109, MI, USA.

<sup>2</sup> Institut für Theoretische Physik J.W.G-Universität Frankfurt, Robert-Mayer-Str. 8 60054 Frankfurt am Main, Germany.

**Abstract.** We present an extensive Quantum Monte Carlo study of the magnetic properties of the mixed-spin quantum systems  $R_2\text{BaNiO}_5$  ( $R$ = magnetic rare earth) which show coexistence of 3-dimensional magnetic long-range order with 1-dimensional quantum gap excitations. We discuss the validity of the performed simulations in the critical region and show the excellent agreement with experimental results. We emphasize the importance of quantum fluctuations contained in our study which is absent in previous mean-field-like treatments.

**PACS.** 75.10.Jm, 75.25.+z, 75.50.Ee

## 1 Introduction

The competition of different orders in mixed-species systems is a subject of actual interest, not only in condensed matter physics where for instance mixed-spin systems have been studied intensively in the last years[1] but also in other research areas like the physics of ultra-cold atomic and molecular gases where Fermi-Bose mixtures are being investigated[2]. The fascination in the mixed-species systems is that they have a very rich phase diagram with coexistence of different orders what leads to interesting competing effects.

Here we want to concentrate on the magnetic behavior of a class of mixed-spin quantum systems,  $R_2\text{BaNiO}_5$  ( $R$ =magnetic rare earth) which show coexistence of 3-dimensional (3D) magnetic long-range order with 1-dimensional (1D) quantum gap excitations [3]. In a previous publication [4] we proposed a microscopic model in order to describe this coexistence of *classical* with *quantum* features in  $\text{Nd}_2\text{BaNiO}_5$  which we evaluated with the Quantum Monte Carlo (QMC) method. In the present article we extend our previous work to the region of critical behavior of the whole family  $R_2\text{BaNiO}_5$  and present a detailed analysis of the QMC simulations which was not included in [4].

The  $R_2\text{BaNiO}_5$  systems have two types of spin carriers i.e.  $S = 1$   $\text{Ni}^{2+}$  ions which form antiferromagnetic chains running along the  $a$  axis of the crystal structure and  $s = \frac{1}{2}$   $\text{R}^{3+}$  ions ( $R$ = rare-earth), positioned between the chains. While perfect isolated  $S = 1$  chains will behave as a Haldane system [5] with no long-range order even at  $T = 0$  and a gap in the magnetic excitation spectrum, long-range ordering occurs in  $R_2\text{BaNiO}_5$  at low temperatures induced by the magnetic  $s = \frac{1}{2}$   $\text{R}^{3+}$  ions. Inter-

estingly, the semi-classical 3D long-range order (i.e. spin-waves) coexists with quantum Haldane-gap excitations in these systems. This behavior has been intensively studied in recent years both experimentally [3,6], as well as theoretically [3,4,7]. A first attempt to understand this coexistence of classical and quantum orders was done by considering a mean field approach [3,7] for the Ni-chains interaction which proved to be very meaningful to understand the basic phenomenon of coexistence. This type of approach is nevertheless unable to provide a detailed description of the physics involved and one has to invoke the use of a microscopic model which should include the main interactions responsible for the system behavior. In [4] we considered a spin model which describes both the interaction within the  $S = 1$  chains and the interaction between the  $S = 1$  chains and the  $s = \frac{1}{2}$  ions in between the chains in the following way:

$$H = J \sum_{ij} \mathbf{S}_{i,2j} \mathbf{S}_{i+1,2j} + J_c \sum_{ij} S_{i,2j}^z (s_{i,2j-1}^z + s_{i,2j+1}^z) \quad (1)$$

with  $J > 0$  and  $J_c > 0$ ,  $S$  denotes spin 1 and  $s$  denotes spin  $1/2$ . The index  $i$  runs along the chain direction and  $j$  in the direction perpendicular to the chains. In Fig. (1) we show a schematic representation of the lattice model. We note that the coupling between  $S=1$  and  $s=1/2$  ions has been chosen Ising-like since neutron scattering experiments[8] on these compounds show that the excitations associated with the rare earths are dispersionless, what indicates that the coupling between the Ni and R sublattices must be extremely anisotropic and can therefore be approximated by an Ising-type term.

Even very simple, minimal models are hard to evaluate and one has to either consider some limiting assumptions

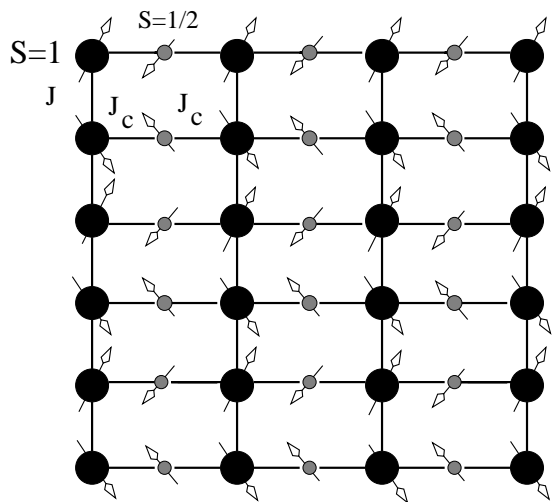


**Fig. 1.** Lattice picture of the model considered for  $R_2\text{BaNiO}_5$  where the big (small) circles correspond to the  $S = 1$  Ni spins ( $s = \frac{1}{2}$  R spins) respectively.  $J$  and  $J_c$  are the Ni-Ni and the Ni-R exchange couplings respectively.

in order to be able to solve the model analytically or make use of numerical simulations, which may prove very accurate for certain models and properties. In our case, we consider the Quantum Monte Carlo (QMC) Method.

The Hamiltonian (1) has been elaborated in such a way that its physical properties are, by construction, in qualitative agreement with a wide range of observations gathered in the family of rare earth nickelates  $R_2\text{BaNiO}_5$ . It has been shown [4] that quantitative agreement to experimental results for  $\text{Nd}_2\text{BaNiO}_5$  can also be achieved by selecting the appropriate value of  $\frac{J_c}{J}$ . A first instance of this agreement is the ratio between the two basic energy scales involved in the problem: i.) The intrinsic gap  $\Delta$  of the system of independent  $S=1$  chains (when  $J_c = 0$ ) and ii.) the Néel temperature  $T_N$  of the complete system when the coupling Ni-Nd is switched on.

In the well-studied  $\text{Y}_2\text{BaNiO}_5$  [9], the rare-earth  $\text{Y}^{3+}$  is non-magnetic and no indication of 3D long-range order has been observed, what strongly suggests that the system can be described by well isolated  $S=1$   $\text{Ni}^{2+}$  chains with a Haldane gap  $\Delta \sim 127\text{K}$ . In the magnetic  $\text{Nd}_2\text{BaNiO}_5$  [10,11,12] the Néel ordering is at  $T_N = 49\text{K}$ . Using these quantities we get a ratio  $r = \frac{\Delta}{T_N} = 2.59$ . Analogously, the gap value of an independent  $S=1$  chain is given uniquely in terms of the exchange constant  $\Delta = 0.410J$ . For  $J_c = 0.31J$ , we find that the ordering temperature is  $T_N = 0.163J$  which gives  $r = 2.51$  (a 3% difference with respect to the experimental value). Furthermore, for the same value of the transverse coupling  $J_c = 0.31J$ , the staggered magnetization for the Ni sublattice  $M_{\text{Ni}}(T \rightarrow 0) = 0.79$  which corresponds to the value  $1.6\mu_B$  observed experimentally. A further validation of this microscopic model was obtained from the comparison of the calculated staggered magnetization as a function of the temperature with the experimental one. Actually, the staggered magnetizations obtained from the QMC computations for both the Nickel ( $M_{\text{Ni}}$ ) and rare earth ( $M_{\text{R}}$ ) sublattices turn out to

be in very good quantitative agreement with the experimental results for  $\text{Nd}_2\text{BaNiO}_5$  [3,4] for  $J_c = 0.31J$ .

Here, based on the model proposed in our previous work [4], we explore the antiferromagnetic/paramagnetic transition of the *whole* family of rare-earth nickelates studied so far  $R_2\text{BaNiO}_5$   $R=\text{Nd,Er,Pr}$  and we propose an effective model for the behavior of these materials in the critical region.

We have organized the paper as follows. In section 2 we describe the QMC algorithm used for our calculations and the data analysis procedure. In section 3 we present the critical temperatures of the microscopic model evaluated with QMC and we compare them with the prediction given by the staggered mean field approach proposed by Zheludev *et al.* [3,7]. An effective model for the critical behavior is presented in section 4 and the QMC result for the spin-spin correlations in the paramagnetic phase in section 5.

## 2 Method and data analysis

To study numerically the Hamiltonian (1) we have used the Loop Algorithm [13] (see also [14] for an extensive review), a variant of the QMC method. This method belongs to the family of quantum cluster algorithms and provides a very efficient prescription for the sampling process of the configuration space. The key for the success of these methods is the following. An accurate simulation of a spin system requires to gather a large sample of (nearly) statistically independent spin configurations in which we measure the physical magnitudes of interest. A simple procedure to collect a sample of spin configurations is by performing local updates involving a few spins in each Monte Carlo step. However, if the correlation length is sizeable, the number of Monte Carlo steps necessary to decorrelate two spin configurations (also called autocorrelation time) is large. To avoid such slowing down, it is necessary to perform global updates involving clusters of spins with a size of the correlation length which: a) preserve all the symmetries of the hamiltonian, b) keep the system near equilibrium. The Loop algorithm gives an efficient prescription for constructing such clusters. In this way the autocorrelation time is of order one ( i.e. a single Monte Carlo step generates a new spin configuration which is nearly independent from the previous one). This is especially important since we are interested also in critical properties where the correlation length is of the size of the system.

The fact that the coupling between  $S=1$  and  $s=1/2$  is of Ising type and not Heisenberg simplifies substantially the implementation of the algorithm. On the other hand, the Hamiltonian (1) is not frustrated and does not show the sign problem, therefore all Boltzmann weights appearing in the evaluation of thermodynamic properties can be taken positive after the conventional rotation around the  $z$ -axis of all the spins in one of the two sublattices of the  $S=1$  system. The temperatures of interest for comparison with experiment are, as we will see, well inside the scope of our QMC method.

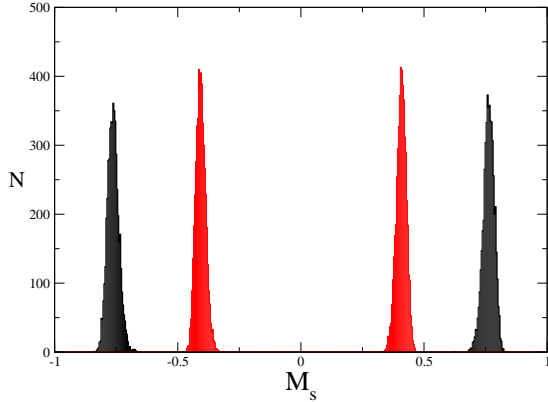


**Fig. 2.** Histograms of the magnetization in the ordered phase for both sublattices and  $J_c = 0.31$  and  $T = 0.1J$ . The black (grey) histogram corresponds to the  $S=1$  ( $s=1/2$ ) species.  $N$  is the number of Monte Carlo measurements of the staggered magnetization giving as a result  $M_s$  after thermalization. The figure suggests that the model has two ground states.

The QMC simulations were performed on finite lattices and we carried out a finite size scaling in order to be able to compare with experiments and we considered periodic boundary conditions  $\mathbf{S}_{L+1,2j} = \mathbf{S}_{1,2j}$  and  $\mathbf{S}_{i,2j} = \mathbf{S}_{i,1}$ . In order to illustrate the finite size analysis, in Figure (2) we show the distribution of the staggered value of the magnetization after  $10^5$  Monte Carlo steps.

Since the model has two ground states in the two sublattices in the ordered phase related by the  $Z_2$  symmetry (see Fig.(2)), the staggered magnetization was computed by taking the absolute value of the staggered component of the spin operator in each Monte Carlo step in order to avoid averaging between configurations around these two ground states, and then using the relation

$$M_{Ni} = \lim_{L \rightarrow \infty} \frac{4}{L^2} \sum_{N_{MC}} \left| \sum_{ij} (-1)^i S_{i,2j} \right|$$

$$M_{Nd} = \lim_{L \rightarrow \infty} \frac{4}{L^2} \sum_{N_{MC}} \left| \sum_{ij} (-1)^i S_{i,2j-1} \right|$$

where  $N_{MC} = 10^5$  is the number of Monte Carlo steps after thermalization. In principle, we considered for this extrapolation  $L \times L$  lattices of size  $L=8, 16, 24, 32, 48, 64$  spins, where  $L$  is the total number of spins including both magnetic species.

In Fig. (3) we show the magnetization in the rare-earth sublattice as a function of the inverse size of the system for a model with  $J_c = 0.36J$  where  $T_N = 0.183J$ . We observe that for temperatures slightly above  $T_N$ , i.e. in the paramagnetic phase, very large lattices are necessary to extrapolate the correct value of the magnetization (zero in this case). However, the extrapolation is an issue only at temperatures very close to the  $T_N$ . As we will see, for comparison with experiments we need to compute the staggered magnetization at temperatures clearly smaller than  $T_N$  where extrapolation is straightforward. Actually,

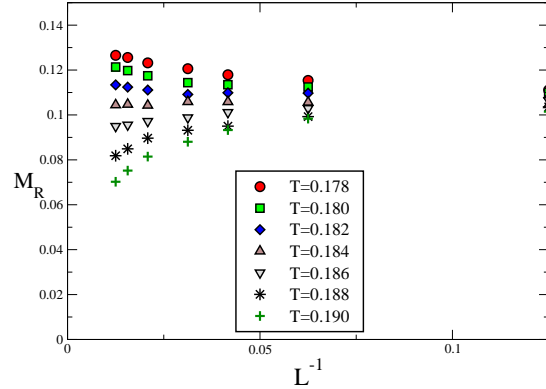


**Fig. 3.** Magnetization in the rare-earth sublattice as a function of the inverse size of the system for temperatures very close to the Néel temperature  $T_N \sim 0.183$  in units of  $J$ . The value of the transverse coupling here is  $J_c = 0.36J$ . Note that the  $T = 0.184$  and  $T = 0.186$  seem to be in the paramagnetic phase which is only observable in very large lattices ( $M_R \rightarrow 0$  as  $L \rightarrow \infty$ ).

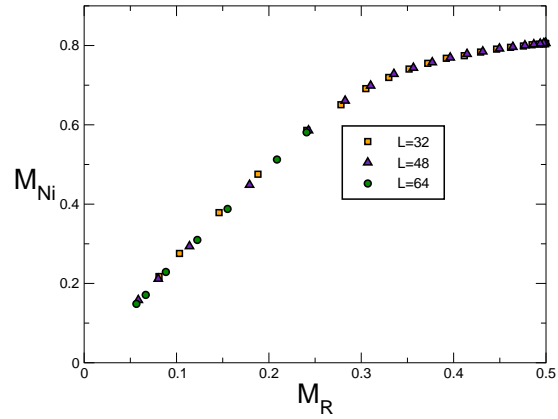


**Fig. 4.** Staggered magnetizations in both sublattices for different values of  $L$ . Far from the critical point, where the correlation length is small, the extrapolation is straightforward. For a given system size each point corresponds to a different temperature in the ordered regime  $T < T_N$ .

that is what we see in Figure (4) where the relation between the staggered magnetizations in both sublattices for different  $L$  values is shown. In this case the staggered magnetization data may already have converged with lattices as small as  $32 \times 32$ .

The Néel temperature was determined by using the Binder parameter [15]  $g$ , which is the fourth cumulant of the order parameter distribution.

$$g = \frac{3}{2} \left( 1 - \frac{\langle M^4 \rangle}{\langle M^2 \rangle^2} \right) \quad (2)$$

At  $T_N$  this cumulant is independent of the size of the system, apart from subdominant corrections to the critical scaling. In Fig. (5) we present the typical finite-size scaling

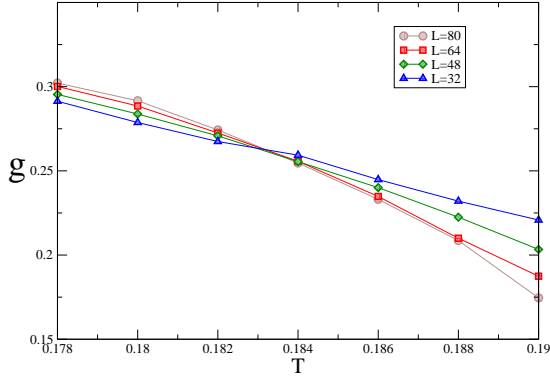


**Fig. 5.** Binder Parameter  $g$  as a function of the temperature for  $J_c = 0.36$ . The line intersection for different system sizes signals the Néel temperature.

for the Binder parameter for  $J_c = 0.36J$  computed in lattices of sizes  $L=24, 32, 48, 64$  spins where the intersection for different system sizes signals the Néel temperature. The data for  $L=8, 16$  show consistently significant subdominant corrections and they were not included in the computation of  $T_N$ . We suspect that this is a consequence of the complex structure of the higher energy excitations, probably Haldane excitations in the  $S=1$  sector surviving in the vicinity of the Néel temperature, what sets another lengthscale  $\xi_{ch} \sim 6$  slightly smaller than the correlation length of an independent  $S=1$  Heisenberg chain. Actually, as we will see below, the energy scale associated to these excitations (the “gap”) increases as we increase  $J_c$ . Therefore only sizes  $L \gg \xi_{ch}$  should enter the finite size analysis [16].

### 3 Numerical simulations vs. mean field approach in the critical regime

The critical properties deserve special attention because the effective staggered field approach proposed by Zheludev *et al.* [3, 7] -being a mean field approximation- can break down in the vicinity of the critical region, i.e. at the Néel temperature. The idea of the mean field is that the behavior of the  $R_2\text{BaNiO}_5$  compounds in the ordered phase can be described in terms of a  $S = 1$  chain of Ni ions in a staggered magnetic field induced by the magnetic rare earth ions:

$$M_{\text{Ni}} = \mathcal{M}(\alpha M_{\text{R}}) \quad (3)$$

where  $\mathcal{M}(h)$  is the staggered magnetization of a  $S=1$  spin Heisenberg chain as a function of the external staggered magnetic field  $h$  induced by the  $s=1/2$  ions and  $\alpha$  is the proportionality constant. Inversely, the otherwise free spins  $s = \frac{1}{2}$  see the mean-field produced by the neighboring  $S = 1$  chains. The staggered magnetization of the R lattice is then related to the staggered magnetization of the Ni lattice by the expression.

$$M_{\text{R}} = M_0 \tanh(\alpha \beta M_{\text{Ni}}) \quad (4)$$

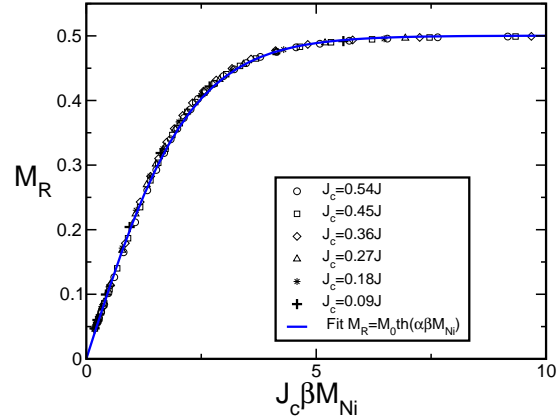


**Fig. 6.** Functional dependence of the QMC results for  $M_{\text{R}}$  vs.  $M_{\text{Ni}}$  for various values of the coupling constant  $J_c$ . The solid lines correspond to Eq. (4).

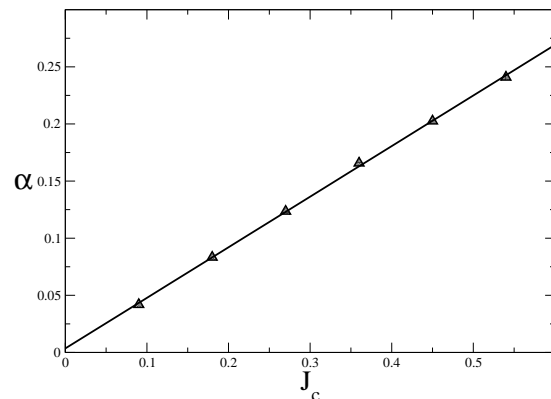


**Fig. 7.** Effective coupling  $\alpha$  between the two sublattices as a function of the Ni-R coupling as obtained from the fits in Fig. 6 The solid line is a fit to the linear law  $\alpha = 0.443J_c + 0.0034$ .

where  $M_0$  is the effective moment of the rare earth ion and  $\beta = 1/k_B T$ .

We aim now to compare our QMC numerical results with the predictions for  $T_N$  of the staggered mean field approach. The coupling between the two sublattices in the staggered mean field formalism is encoded in the constant  $\alpha$  instead of the microscopic coupling constant  $J_c$ . Therefore the first step is to find a relation between both in the antiferromagnetic phase. In Fig. (6) we present the QMC results for  $M_{\text{R}} = f(J_c \beta M_{\text{Ni}})$  for various values of  $J_c$ . Note that all curves fall on top of each other and, in fact, this curve can be described by Eq. (4) where  $\alpha$  must be a linear function of  $J_c$  in the range of transverse couplings studied as observed from our QMC results. Furthermore, we have extracted the relation  $\alpha = 0.0034 + 0.443J_c$  in that range, which can be considered linear within our statistical error bars (see Figure 7).

At this point it is legitimate to question the relation between a microscopic coupling  $J_c$  and a frankly phenomenological constant  $\alpha$  especially at finite temperatures. Since

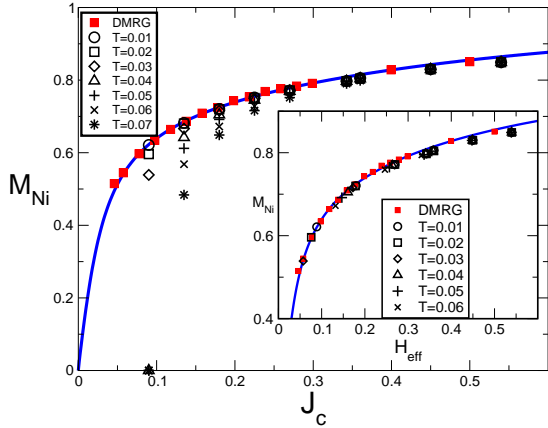


**Fig. 8.**  $M_{\text{Ni}}$  vs. the value of the  $J_c$  for several values of  $J_c$  and temperatures in units of  $J$ . In the inset  $M_{\text{Ni}}$  vs. the 'effective' field on the Ni-subsystem induced by  $M_{\text{R}} H = 2J_c M_{\text{R}}$  [3] for various  $T$  values. The squares correspond to the DMRG results [17] at  $T=0$ .

our QMC data are collected in the range of temperatures  $T_{\text{min}} < T < T_N$ , where  $T_{\text{min}}$  was the minimal energy that we were able to simulate, it is necessary to study whether there is a temperature dependence in  $\alpha$ . In the main picture of Fig. (8) we show the relation between  $M_{\text{Ni}}$  and the value of the transversal coupling  $J_c$  at various temperatures. Actually the data converge in the  $T=0$  limit to a well defined curve  $M_{\text{Ni}}(J_c)$  which at low values of  $J_c$  is the magnetization curve of the 1D  $S=1$  Heisenberg model at  $T=0$  in a staggered magnetic field computed by Yu *et al.* [17] using the Density Matrix Renormalization Group (DMRG) method.

In the inset of Fig. (8) we directly plot  $M_{\text{Ni}}$  vs.  $H_{\text{eff}}$  for various  $T$  values assuming that  $\alpha$  is temperature independent. Now we have that even when the staggered magnetization in the R lattice is not at saturation we find that the rescaled data are superimposed to the magnetization curve of the 1D  $S=1$  Heisenberg model at low values of  $J_c$ . This data collapse is a consequence of the large value of the Haldane gap and the low temperatures considered. At higher values of  $J_c$ , the R sublattice remains nearly saturated at the highest values of the  $T$  considered ( $T=0.07J$ ), therefore no difference is observed when the rescaling is done. The results presented in Fig. (8) also confirm that the assumption of a temperature independent  $\alpha$  is valid in the range of temperatures considered and that the mean field approach works very well if the chains are weakly coupled to the R magnetic moments but there are small deviations at higher values of  $J_c$ . Analyzing the QMC results, the scale that separates the 1D from the 2D regime is the Haldane gap  $H_{\text{eff}} \sim \Delta_{1D} \sim 0.41J$  as expected. We also note that for the smallest value of  $J_c$ ,  $J_c = 0.09J$  the Néel temperature is so small  $T_N = 0.06J$  that some of the points are still in the paramagnetic phase  $M_{\text{Ni}}(T) = 0$ .

In addition, to corroborate the relevance of the quantum fluctuations in this system, we present in Fig. (9) a

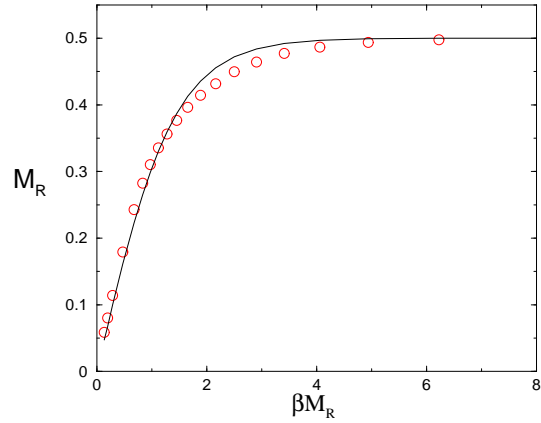


**Fig. 9.** Classical mean-field (solid line) compared to QMC results (open circles). Note that a classical mean field theory approach fails to correctly relate the staggered magnetization in any sublattice. Here we show the best possible fit using the rare-earth subsystem.

comparison of a classical mean field model of the staggered magnetization in the R sublattice i.e.  $M_{\text{R}}$  as a function of  $\beta M_{\text{R}}$  and independent of the magnetization of the Ni sublattice (solid line) (Brillouin function) with the QMC data obtained with the Hamiltonian (1) (open circles). We observe that there is a significant deviation between the data and the Brillouin function which can be attributed to the effect of the quantum fluctuations on the magnetization in the R sublattice which are contained in the model Eq. (1) but not in a classical mean field model.

A numerical solution of Eqs. (3-4) in the whole AFM phase ( $0 \leq M_{\text{R}} \leq 0.5$ ,  $0 \leq M_{\text{Ni}} \leq 1.0$ ) demands an explicit analytic expression for the staggered magnetization as a function of the external staggered magnetic field in a  $S=1$  chain. For that purpose we took the DMRG results of Ref. [17] and got the best possible fit. The only conditions that we impose to our fitting function are: i) It should have a smooth fitting behavior in the wide range of values necessary to the numerical solution of (3-4) ii) it should show linear behavior at low external fields and iii) it should have asymptotic saturation at high external fields. The explicit expression that we obtained was:

$$M = A \arctan(Bh) + C \tanh(Dh) + Eh/(1 + Eh); \quad (5)$$

where  $A=0.177457$ ,  $B=9.58055$ ,  $C=0.336168$ ,  $D=56.5282$  and  $E=0.386596$ . The equations (3-4) can be solved now numerically confirming in general the excellent agreement of QMC and the mean field in the ordered phase but there is *qualitative* disagreement in the  $T_N(J_c)$  relations as shown in Fig. (10). In Fig. (10) we compare the Néel temperature as a function of  $J_c$  obtained numerically (triangles) using the Binder parameter as explained in the previous section with the mean field solution (dashed line). The most significant feature of the mean field solution is its quadratic behavior in  $\alpha$  and therefore in  $J_c$ . This result suggests that the functional relation between  $\alpha$  and  $J_c$

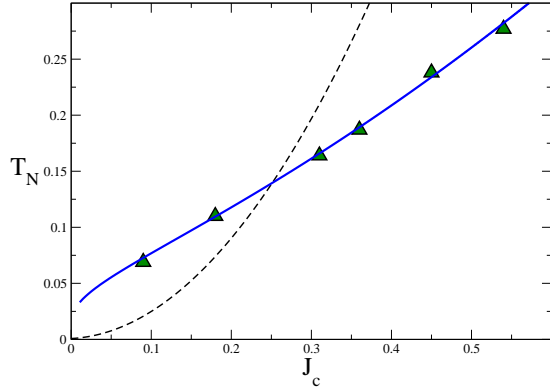


**Fig. 10.** Néel temperature as a function of the Ni-R coupling  $J_c$  in units of  $J$ . The triangles are the result of our QMC simulation in our model Hamiltonian. The dashed line is the mean field result given by the equations (4-3) and the solid line is the fit to a 2D anisotropic Ising model (see text).

changes abruptly close to the critical point and  $\alpha \sim \sqrt{J_c}$  would be more appropriate in that regime. We shall investigate this discrepancy in more detail in the next section.

## 4 Effective description of the critical behavior

Our purpose here is to reproduce the relation  $T_N(J_c)$  (see Fig. (10)) using a model that includes the critical fluctuations that seem to be missing in the mean field approach.

To elaborate such a model let us consider the following observations:

i.) The magnetic moments in the rare earth commute with the total Hamiltonian

$$[s_{i,2j\pm 1}^z, H] = 0 \quad (6)$$

which implies that  $M_R$  is a good quantum number of the Hamiltonian irrespective of the value of  $J_c$ .

ii.) At finite temperatures the model has two ground states related by the  $Z_2$  symmetry in both sublattices as shown in the histograms of the magnetization in the ordered region (see Figure (2) where the distribution of the order parameter is presented after thermalization.)

iii.) The spin rotational invariance has been broken by the Ising character of  $J_c$ . As predicted by Haldane [5] and elaborated on microscopical grounds by Gomez-Santos [18], the low-energy sector of the XXZ  $S=1$  Heisenberg chain can be mapped onto a 2D Ising model. Actually, the longitudinal spin-spin correlation function of a Haldane chain is identical to the one of the 2D Ising model in the paramagnetic phase, including the power-law correction to the scaling. The previous relation is an example of mapping a quantum model in dimension  $d$  to a classical model in  $d+z$  dimensions, where  $z=1$  for this case. The length of the imaginary time dimension is determined by the inverse temperature  $\beta$ .

Let us consider then a system of Ising planes coupled by the intercalated moments of the rare-earth. In the ma-

terials of interest we have always  $T_N < \Delta$ . In the paramagnetic phase  $T_N < T < \Delta$  we expect that the autocorrelation time  $\xi_T$  in the imaginary direction to be smaller than  $\beta$  and the system behaves effectively as a three dimensional Ising model. As the temperature is reduced, a crossover takes place when  $\xi_T$  becomes of the order of  $\beta$ . Beyond that point the system belongs to the 2D Ising model universality class with different coupling constants in the two spatial dimensions.

The simplest effective model (i.e. valid in the vicinity of the critical point) and compatible with the arguments above is an anisotropic 2D Ising model whose critical temperature is given by the Kramers-Wannier expression [19]:

$$\sinh(2J_{\parallel}/T_N) \sinh(2J_{\perp}/T_N) = 1 \quad (7)$$

where  $J_{\parallel} = 2.35$  and  $J_{\perp} = 0.022J_c^2$  are the effective couplings of the model. In Fig. 10 we show the agreement of this effective model (solid line) with the QMC data obtained for Eq. (1) (triangles).

## 5 The paramagnetic phase

For completion, we present in this section the spatial spin-spin correlations in the paramagnetic phase. At  $T = T_N$  the spin-spin correlation function decays algebraically and therefore the correlation length is infinite. As the temperature increases, the correlation length decreases. If the nominal gap  $\Delta$  of the independent  $S=1$  is large enough, the properties of the independent  $S=1$  should become visible in the paramagnetic phase. The question we are interested in is whether this crossover is observable in the value of the correlation length.

In Figures (11) and (12) we present the correlation functions of the z-component of the spin operators in the Ni and R sublattice respectively. We observe that, even though the R-R correlations are two orders of magnitude smaller than the Ni-Ni correlations, there are finite correlations between the  $s=1/2$  spins mediated by the chains. We recall that the model doesn't couple the  $s=1/2$  spins directly. The immediate question is: which is the induced correlation length between the rare earth magnetic moments?

Following White and Huse [20], we calculated the correlation length  $\xi$  for both sublattices in a  $64 \times 64$  spins lattice by fitting the z-component of the spin-spin correlation function to the law:

$$|\langle S_0^z S_l^z \rangle| = A \exp\left(\frac{-l}{\xi}\right) l^{-\eta} \quad (8)$$

where  $A$  and  $\eta$  are fitting parameters. In the vicinity but not too close to  $T_N$  we find a fit of the correlation length temperature to a power law in both sublattices. We took values in a range  $\xi \sim 5 - 17$  that can be accurately computed with the procedure described above. The best fit is  $\xi^{-1} = K(T - T_N)^{\frac{1}{2}}$  where  $K$  is the only free parameter[4]. Such behavior is the one expected for a Ginzburg-Landau like description *above* the critical point confirming that a



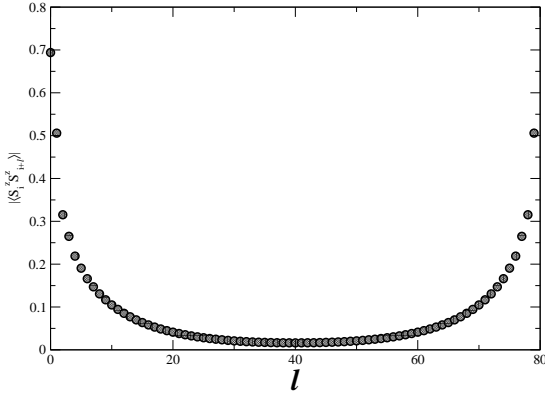


**Fig. 11.** Spin-spin correlation function (z-component) in the Ni subsystem and along the chains ( $J_c = 0.18$ ) in a lattice of  $80 \times 80$  sites

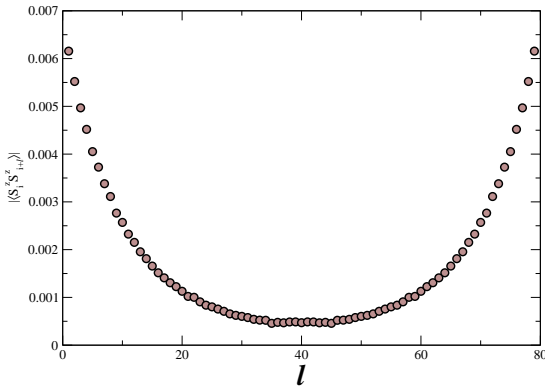


**Fig. 12.** Same magnitudes and parameters as in figure (11) for the R subsystem. Note the change in scale.

mean field description is again valid as we depart from the critical point from above. Besides, we note that for  $T \gg T_N$ , the correlation length in the Ni subsystem approaches the correlation length of a single chain.

The fitting parameter  $\eta$  shows a differentiated temperature dependence in both sublattices i.e  $\eta = 0$  for the correlation function Eq. (8) in the R-sublattice while in the Ni sublattice  $\eta$  approaches the value 0.5 as the temperature is reduced in the paramagnetic phase.

## 6 Conclusions.

In conclusion, we have provided a detailed analysis of the antiferro-/paramagnetic transition of the  $R_2BaNiO_5$  mixed-spin quantum antiferromagnets based on QMC simulations of a lattice model of interacting spin-1 and spin-1/2 entities. We give an extensive description of the numerical calculations and data analysis and comparison of our results with experimental observations is very good. These calculations go beyond previous mean field type of

approaches and retain the main features of the behavior of the system in the critical region. We propose an effective 2D anisotropic Ising model to explain the behavior of the Néel temperature as a function of the coupling between the nickel and the rare earth sublattices.

## 7 Acknowledgements.

It is a pleasure for us to acknowledge discussions with C. Gros, S. Moukouri, H. Rieger and A. Zheludev.

## References

1. see J.V. Alvarez, H. Rieger and A. Zheludev, Phys. Rev. Lett. **93**, 156401 (2004) and references therein
2. see M. Lewenstein, L. Santos, M. A. Baranov, and H. Fehrmann, Phys. Rev. Lett. **92**, 050401 (2004).
3. A. Zheludev, E. Ressouche, S. Maslov, T. Yokoo, S. Raymond, J. Akimitsu Phys. Rev. Lett. **80**, 3630 (1998).
4. J.V. Alvarez, R. Valentí, and A. Zheludev, Phys. Rev. B, **65**, 184417 (2002).
5. F.D.M. Haldane, Phys. Rev. Lett. **50**, 1153 (1983).
6. S. Raymond, T. Yokoo, A. Zheludev, S. E. Nagler, A. Wildes and J. Akimitsu, Phys. Rev. Lett. **82**, 2382 (1999).
7. A. Zheludev, S. Maslov, T. Yokoo, S. Raymond, S. E. Nagler and J. Akimitsu J. Phys.: Condens. Matter **13**, R525 (2001).
8. S. Maslov and A. Zheludev, Phys. Rev. Lett. **80**, 5786 (1998).
9. J. Darriet and L. P. Regnault, Solid State Commun. **86**, 409 (1993); T. Yokoo, T. Sakaguchi, K. Kakurai and J. Akimitsu, J. Phys. Soc. Japan **64**, 3651, (1995); G. Xu, J. F. DiTusa, T. Ito, K. Oka, H. Takagi, C. Broholm, G. Aeppli, Phys. Rev. B **54**, R6827 (1996).
10. J.A. Alonso, J. Amador, J.L. Martínez, I. Rasines, J. Rodríguez-Carvajal, R. Saez-Puche, Solid State Commun. **76**, 467 (1990).
11. E. García-Matres, J.L. Martínez, J. Rodríguez-Carvajal, A. Salinas-Sánchez, Solid State Commun. **85**, 553 (1993).
12. A. Zheludev, J. M. Tranquada, T. Vogt, D. J. Buttrey, Phys. Rev. B. **54**, 7210 (1996).
13. H.G. Evertz, G. Lana and M. Marcu, Phys. Rev. Lett. **70**, 875 (1993)
14. H.G. Evertz, Adv.Phys. **52**, 1 (2003)
15. *Monte Carlo Simulations in Statistical Physics* D. P. Landau and K. Binder (Cambridge University Press, 2000).
16. Calculations are done in units  $\mu_B = k_B = \hbar = 1$ .
17. J. Lou, X. Dai, S. Qin, Z. Su, L. Yu. Phys. Rev. B **60**, 52 (1999).
18. G. Gomez-Santos, Phys. Rev. Lett. **63**, 790 (1989)
19. H.A. Kramers and G.H. Wannier, Phys. Rev. **60**, 252 (1941).
20. S. R. White and D. A. Huse, Phys. Rev. B **48**, 3844 (1993).